

Lawrence Berkeley National Laboratory

Recent Work

Title

Comparative genomics of *Rhizophagus irregularis*, *R. cerebriforme*, *R. diaphanus* and *Gigaspora rosea* highlights specific genetic features in Glomeromycotina.

Permalink

<https://escholarship.org/uc/item/96v5r8d4>

Journal

The New phytologist, 222(3)

ISSN

0028-646X

Authors

Morin, Emmanuelle
Miyachi, Shingo
San Clemente, Hélène
et al.

Publication Date

2019-05-01

DOI

10.1111/nph.15687

Peer reviewed

Article type : MS - Regular Manuscript

Comparative genomics of *Rhizophagus irregularis*, *R. cerebriforme*, *R. diaphanus* and *Gigaspora rosea* highlights specific genetic features in *Glomeromycotina*

Emmanuelle Morin¹, Shingo Miyauchi¹, Hélène San Clemente², Eric CH Chen³, Adrian Pelin³, Ivan de la Providencia³, Steve Ndikumana³, Denis Beaudet³, Mathieu Hainaut⁴, Elodie Drula⁴, Alan Kuo⁵, Nianwu Tang², Sébastien Roy⁶, Julie Viala⁶, Bernard Henrissat^{4,7}, Igor V. Grigoriev⁵, Nicolas Corradi^{3*}, Christophe Roux^{2*}, Francis M. Martin^{1,8*}

¹ Institut national de la recherche agronomique, Université de Lorraine, Unité Mixte de Recherche Arbres/Microorganismes, Centre INRA-Grand Est-Nancy, 54280 Champenoux, France;

² Laboratoire de Recherche en Sciences Végétales, Université de Toulouse, UPS, CNRS 24 Chemin de Borde Rouge-Auzeville, 31320 Castanet-Tolosan, France;

³ Department of Biology, University of Ottawa, Ottawa ON K1N 6N5, Canada;

⁴ CNRS, UMR 7257, Aix-Marseille Université, 13007 Marseille, France ;

⁵ US Department of Energy Joint Genome Institute (JGI), Walnut Creek, California 94598, USA;

⁶ Agronutrition- rue Pierre et Marie Curie, Immeuble BIOSTEP 31670 Labège, France ;

⁷ Architecture et Fonction des Macromolécules Biologiques, Aix-Marseille Université, 13007 Marseille, France;

⁸ Beijing Advanced Innovation Center for Tree Breeding by Molecular Design, Beijing Forest University, 100080 Beijing, China.

ORCID :

Emmanuelle Morin 0000-0002-7268-972X

Shingo Miyauchi 0000-0002-0620-5547

Eric CH Chen 0000-0001-5367-7259

Elodie Drula 0000-0002-9168-5214

Bernard Henrissat 0000-0002-3434-8588

Igor V. Grigoriev 0000-0002-3136-8903
Nicolas Corradi 0000-0002-7932-7932
Christophe Roux 0000-0001-5688-5379
Francis M. Martin 0000-0002-4737-3715

*Joint senior authors

Authors for correspondence: Francis Martin: Tel. +33 383 39 40 80; Email: francis.martin@inra.fr; Christophe Roux: Tel. +33 5 34 32 38 04; Email: roux@lrsv.ups-tlse.fr; Nicolas Corradi: Tel: +1 613 562 58 00; Email: ncorradi@uottawa.ca

Received: 23 October 2018

Accepted: 28 December 2018

Total word count (excluding summary, references and legends): 7,102

Abstract: 196 / Introduction: 1,041 / Material and Methods: 2,091 / Results: 2,361 /

Discussion: 1,286 / Acknowledgements: 127

6 color figures (Fig.1, Fig.2, Fig.4, Fig.5, Fig. 6) / 1 table

Supporting Information (6 figures; 17 tables)

1 **Summary**

2 • Glomeromycotina is a lineage of early diverging Fungi establishing arbuscular
3 mycorrhizal (AM) symbiosis with land plants. Despite their major ecological role,
4 genetic bases of their obligate mutualism are largely unknown, hindering our
5 understanding of their evolution and biology.

6 • We compared the genomes of Glomerales (*Rhizophagus irregularis*,
7 *Rhizophagus diaphanus*, *Rhizophagus cerebriforme*) and Diversisporales (*Gigaspora*
8 *rosea*) species, together with those of saprotrophic Mucoromycota, to identify gene
9 families and processes associated with these lineages and to understand the molecular
10 underpinning of their symbiotic lifestyle.

11 • Genomic features in Glomeromycotina appear to be very similar with a very high
12 content in transposons and protein-coding genes, extensive duplications of protein
13 kinase genes, and loss of genes coding for lignocellulose degradation, thiamin
14 biosynthesis and cytosolic fatty acid synthase. Most symbiosis-related genes in
15 *R. irregularis* and *G. rosea* are specific to Glomeromycotina. We also confirmed that
16 the present species have a homokaryotic genome organization.

17 • The high interspecific diversity of Glomeromycotina gene repertoires, affecting all
18 known protein domains, as well as symbiosis-related orphan genes, may explain the
19 known adaptation of Glomeromycotina to a wide range of environmental settings. Our
20 findings contribute to an increasingly detailed portrait of genomic features defining the
21 biology of AM fungi.

22
23 **Key words:** arbuscular mycorrhizal fungi, carbohydrate-active enzymes, fungal
24 evolution, interspecific variation, protein kinases, transposable elements.

25

26 **Introduction**

27 The Glomeromycotina is a division of early diverging Fungi (Mucoromycota sensu
28 Spatafora et al., 2016) with 315 described species ([www.amf-
29 phylogeny.com/amphylo_species.html](http://www.amf-phylogeny.com/amphylo_species.html)). Members of this sub-phylum are able to
30 establish AM symbiosis in association with 71% of land plants (Brundrett and
31 Tedersoo, 2018). The mutualistic relationship established by AM fungi has a substantial
32 impact on growth, development and ecological fitness of plants in natural and
33 agricultural ecosystems (van der Heijden et al., 2015). This symbiotic association
34 emerged over 410 million of years ago (Mya) (Strullu-Derrien et al., 2018), and is
35 considered ancestral in land plant evolution (Spatafora et al., 2016; Martin et al., 2017;
36 Field & Pressel, 2018). It is thought that obligate mutualistic Glomeromycotina derived
37 from saprotrophic ancestors from the Mucoromycota lineage (Spatafora et al., 2016),
38 although different views on the appropriate taxonomic rank of AM fungi are currently
39 present in the research community. Here, we consider that Mucoromycota comprises
40 Glomeromycotina, Mortierellomycotina, and Mucoromycotina and is sister to Dikarya
41 (Spatafora et al., 2016). Despite the fact that the first AM symbionts originated >410
42 Mya, features of their genomes can be reconstructed through phylogenetically-informed
43 comparisons among extant symbiotic Glomeromycotina and saprotrophic
44 Mucoromycota. To harness this potential, genome sequences of divergent
45 Glomeromycotina species with different life histories are needed. To date, only three
46 species of Glomeromycotina have their genome published, namely *Rhizophagus*
47 *irregularis* (Schenck & Sm.) Walker & Schüßler (Tisserant et al., 2013; Li et al., 2014;
48 Chen et al., 2018; Maeda et al., 2018), *R. clarus* (Nicolson & Schenck) Walker &
49 Schüßler (Kobayashi et al., 2018) and *Diversispora epigaea* (Daniels & Trappe) Walker
50 & Schüßler (formerly *Glomus versiforme*) (Sun et al., 2018), meaning that the gene
51 repertoires of most species of Glomeromycotina have yet to be sequenced, analyzed and
52 compared.

53 The strain DAOM197198 of *R. irregularis* was the first Glomeromycotina genome to
54 be sequenced (Tisserant et al., 2013, Lin et al., 2014). This genome showed that
55 *R. irregularis* has substantial phylogenetic relationships with saprotrophic
56 Mortierellomycotina and shares several genetic and metabolomic features with early
57 diverging fungi in Mucoromycotina (Tisserant et al., 2013; Chang et al., 2015;

58 Spatafora et al., 2016; Uehling et al., 2017). It also provided unprecedented insights
59 into molecular bases of the AM symbiosis, sexual reproduction and physiology in an
60 iconic representative of Glomeromycotina. The DAOM197198 genome is homokaryotic
61 with a low nucleotide sequence polymorphism, and one of the largest fungal genomes,
62 with an unusually high content of transposable elements (TE) and a strikingly high
63 number of gene duplications (Tisserant et al., 2013, Lin et al., 2014). DAOM197198
64 experienced the loss of several, otherwise widely conserved Mucoromycotina genes
65 with functions related to cell wall polysaccharide degradation, and overall primary and
66 secondary metabolism which could explain its obligate biotrophy. These features have
67 recently been corroborated by the sequencing of five additional isolates from
68 *R. irregularis* (Chen et al., 2018), *R. clarus* (Kobayashi et al., 2018) and *D. epigaea*
69 (Sun et al., 2018). Most importantly, no gene encoding multidomain de novo fatty acid
70 synthase was detected in the genome of these species as initially suggested by Wewer
71 and co-authors (2014) based on the analysis of *R. irregularis* gene repertoire. Esterified
72 palmitic acid is transferred from plant roots to symbiotic mycelium and this lipid export
73 pathway, together with soluble carbohydrates, contributes a substantial amount of
74 carbon to symbiotic hyphae of *R. irregularis* (Bravo et al., 2017; Luginbuehl et al.,
75 2017).

76 Isolates of *R. irregularis* harvested from the same field harbor a very large variability
77 in their gene repertoire affecting most known cellular and biochemical functions, as
78 well as putative mycorrhiza-induced small secreted effector-like proteins (MiSSPs) and
79 other differentially expressed symbiotic genes with no known function (Chen et al.,
80 2018). High variability is also found in active transposable elements. These findings
81 indicate a substantial divergence in the functioning capacity of *R. irregularis* isolates,
82 and as a consequence, their genetic potential for adaptation to biotic and abiotic
83 changes.

84 Although transcriptomic assemblies were recently obtained from a number of AM
85 fungi (Salvioli et al., 2016; Tang et al., 2016; Beudet et al., 2018), our view of the
86 genomic features of Glomeromycotina subphylum is still highly biased by the fact that
87 they have been obtained with species that shared a last common ancestor with other AM
88 relatives many millions of years ago. As of today, molecular bases of genomic
89 adaptations that facilitated evolutionary processes to the obligate symbiotic lifestyle

90 throughout the Glomeromycotina phylum are unknown and can only be elucidated by
91 using additional full genome sequences from various clades of AM fungi. Acquiring
92 genomic information from additional Glomeromycotina species is also needed to
93 corroborate their genomic idiosyncrasies, the high intraspecific genome diversity found
94 in *R. irregularis* (Chen et al., 2018) and its impact on species delimitation (Bruns et al.,
95 2018).

96 In the present study, we provide a comparative analysis of four genomes of
97 Glomeromycotina symbionts, namely *R. irregularis* DAOM197198, *R. diaphanus*
98 (Morton & Walker) Walker & Schüßler MUCL43196, *R. cerebriforme* DAOM227022
99 in Glomales and *Gigaspora rosea* Nicolson & Schenck DAOM194757 in
100 Diversisporales. Genomes of *R. diaphanus*, *R. cerebriforme* and *Gigaspora rosea* have
101 been sequenced and annotated for this study as they belong to the more diversified
102 Glomeromycotina clades (Redecker et al., 2013) and they also present contrasted
103 developmental, ecological and symbiotic traits (Bonfante and Genre, 2008). Our aims
104 are to assess whether the known genome features of *R. irregularis* are shared by other
105 clades of AM fungi and to provide new insights into the evolutionary genome dynamics
106 of the genome in the ancestral lineage leading to Glomeromycotina at two broad levels:
107 gene family origin and diversification, and conservation of gene repertoire features. Our
108 analysis focuses on inter-species genome diversity in key gene categories involved in
109 symbiosis development and functioning and differential gene family expansion and
110 contraction. We also confirm the occurrence of genes potentially related to mating in
111 these supposedly ancient clones and a low genetic diversity among their co-existing
112 nuclei. Comparison of AM fungal genomes with those of *Mortierella elongata*
113 (*Mortierellomycotina*) and representative *Mucoromycotina* species indicates extensive
114 copy number variations in genes involved in nutrient acquisition, developmental
115 pathways, and primary and secondary metabolism. This study, together with the recent
116 analyses of Chen et al. (2018), Kobayashi et al. (2018), Maeda et al. (2018) and Sun et
117 al. (2018), have expanded and refined our understanding of the genomic heritage of AM
118 symbionts.
119

120 **Methods and Materials**

121 Production of fungal materials

122 Spores and mycelium of *R. irregularis* DAOM197198 (aka DAOM181602) and
123 *G. rosea* DAOM194757, produced on carrot root organ cultures, were obtained from
124 Agronutrition (Labège, France). Carrot root organ cultures of *R. diaphanus*
125 MUCL 43196 and *R. cerebriforme* DAOM227022 were obtained from the
126 Glomeromycota in vitro Collection (GINCO) located at Agriculture Canada (Ottawa,
127 Canada).

128

129 De novo genome assembly

130 High molecular weight genomic DNA of *R. irregularis*, *R. diaphanus*, *R. cerebriforme*
131 and *G. rosea* was extracted from large amounts of mycelium produced on carrot root
132 organ cultures as described in Tisserant et al. (2013) and Ropars et al. (2016). DNA was
133 used to construct paired-end (2 x 125 bp) TruSeq Nano libraries and mate-pair libraries
134 (with insert sizes of 3 and 8 kbp) using Nextera Mate Pair Sample Prep Kit. Libraries
135 were sequenced using the Illumina HiSeq 2500 platform (Illumina, Inc., San Diego,
136 CA, USA) at the GeT-PlaGe sequencing facility (Toulouse, France). Low quality
137 sequences and sequencing adapters were trimmed from the raw Illumina reads using
138 Trimmomatic (Bolger et al., 2014). The adapter sequences on mate-pair sequences were
139 removed using the software Nextclip with default parameters (Leggett et al., 2014).
140 Sequences were assembled using AllPathsLG version 43460 (Gnerre et al., 2011) as
141 described in Chen et al. (2018). Scaffolds were queried against the NCBI's
142 nonredundant nucleotide database by using BLASTn and sequences with >90% identity
143 and 75% coverage to plant or bacterial sequences were considered as contaminants and
144 removed. Sequences with a GC%>45 were also considered as bacterial contaminants
145 and discarded (Tisserant et al., 2013). The putative MAT-loci of *Paraglomus* sp.,
146 *Claroideogloium claroideum*, *Gigaspora rosea*, *Scutellospora castanea* and *Glomus*
147 *macrocarpum* were identified along preliminary genome surveys of these species using
148 reciprocal BLAST procedures (Ropars et al. 2016).

149

150 Genome annotation
151 Gene prediction and functional annotation (Gene Ontology (GO), Eukaryotic
152 Orthologous Groups of Proteins (KOG), Kyoto Encyclopedia of Genes and Genomes
153 (KEGG), proteases (MEROPS database) have been carried out using the Joint Genome
154 Institute (JGI) Annotation Pipeline. This bioinformatic pipeline detects and masks
155 repeats and transposable elements (TE), predicts genes, characterizes each conceptually
156 translated protein, chooses a best gene model at each locus to provide a filtered working
157 set, clusters the filtered sets into draft gene families and creates a JGI Genome Portal at
158 the MycoCosm database with tools for public access and community-driven curation of
159 the annotation (Grigoriev et al., 2014). The quality of the draft assemblies was
160 evaluated by using conserved fungal proteins with Benchmarking Universal Single-
161 Copy Orthologs (BUSCO version 3.0.2; Simão et al., 2015). We used default parameter
162 values, the fungal BUSCO set (Fungi odb9 gene set; [http://buscodev.ezlab.org/datasets/
163 fungiodb9.tar.gz](http://buscodev.ezlab.org/datasets/fungiodb9.tar.gz)), and performed searches with HMMER version 3.1. Carbohydrate-
164 active enzymes, so-called CAZymes, including glycoside hydrolases (GH), glycosyl
165 transferases (GT), polysaccharide lyases (PL), carbohydrate esterases (CE), enzymes
166 that act in conjunction with other CAZymes (Auxiliary activities, AA), carbohydrate-
167 binding modules (CBM) and enzymes distantly related to plant expansins (EXPN), were
168 identified using the CAZy database (www.cazy.org) annotation pipeline (Lombard et
169 al., 2014). Secreted proteins were identified using a custom pipeline including SignalP
170 v4, WolfPSort, TMHMM, TargetP, and PS-Scan algorithms as reported in Pellegrin et
171 al. (2016).

172 Prediction of transposable elements (TE) was carried out as described in Payen et al.
173 (2017). De novo repeat sequences were identified in unmasked genome assemblies,
174 downloaded from JGI MycoCosm (Grigoriev et al., 2014), using RepeatScout 1.0.5
175 with default parameters (sequences ≥ 50 bp, ≥ 10 occurrences) (Price et al., 2005).
176 Filtered sequences were annotated by searching homologous sequences against the
177 fungal references in RepBase version 22.08
178 (<http://www.girinst.org/server/RepBase/index.php>) using tBLASTx (Altschul et al.,
179 1990). The coverage of TE, including unknown categories, in genomes was estimated
180 by masking the genome assemblies using RepeatMasker open 4.0.6
181 (<http://www.repeatmasker.org>). Output files generated from the procedures above were

182 integrated, the genome size and repeat element coverage were calculated, and the results
183 were visualised using a set of custom R scripts named Transposon Identification
184 Nominative Genome Overview (TINGO) (available on request).

185 The putative MAT-loci have been deposited in GenBank and are available under the
186 accession numbers MH445370 to MH445379. The new genome assembly and
187 annotation from *R. irregularis* DAOM197198 have been published in Chen et al.
188 (2018), whereas genome assemblies from *R. diaphanus* MUCL43196 and
189 *R. cerebriforme* DAOM227022 have been published in Ropars et al. (2016). The
190 genome assembly of *G. rosea* DAOM194757 has been produced for this study.

191
192 RNA extraction, sequencing and expression analysis

193 For gene expression profiling, all biological samples were produced in triplicates.
194 Spores of *R. irregularis* DAOM197198 and *G. rosea* DAOM194757 were germinated
195 during seven days in liquid M medium (Bécard and Fortin, 1988) in the dark at 30°C
196 with 2% CO₂. Transcripts from these germinating hyphae were used as reference (non-
197 symbiotic control) for calculating the gene expression ratio. Intraradical mycelium of
198 *R. irregularis* and *G. rosea* colonising *Brachypodium distachyon* genotype Bd21 were
199 collected from pot cultures (see Kamel et al. (2017) for details).

200 Total RNA extraction, sequencing procedure and expression analyses were
201 performed according to Tisserant et al. (2011) for *R. irregularis*, and Tang et al. (2016)
202 and Kamel et al. (2017) for *G. rosea*. In brief, one to three µg of total RNA was
203 extracted from germinating hyphae and mycorrhizal roots using the RNeasy Plant Mini
204 RNA Extraction Kit (Qiagen, Germany) and stored at -80°C until further analysis.
205 cDNA library construction and sequencing were performed at the GeT-PlaGe
206 sequencing facility according to standard Illumina protocols. Bioinformatic procedures
207 for transcript profiling were detailed in Kamel et al. (2017): trimmed paired-end reads
208 were mapped onto predicted genes from *R. irregularis* (genome assembly Rhiir2_1) and
209 *G. rosea* (genome assembly Gigro1) using CLC Genomics Workbench (Qiagen) with
210 stringent settings (similarity and length read mapping criteria at 98% and 95%,
211 respectively). Total mapped paired-end reads for each gene were calculated and total
212 read counts were normalized as fragments per kilobase of gene model per million
213 fragments mapped (FPKM). Detailed description of the RNA-Seq analysis (i.e.,

214 specifying reads and reference, defining read mapping options, calculating expression
215 values) can be found in the CLC Workbench online manual at:
216 [http://resources.qiagenbioinformatics.com/manuals/clcgenomicsworkbench/950/index.p](http://resources.qiagenbioinformatics.com/manuals/clcgenomicsworkbench/950/index.php?manual=RNA_Seq_analysis.html)
217 [hp?manual=RNA_Seq_analysis.html](http://resources.qiagenbioinformatics.com/manuals/clcgenomicsworkbench/950/index.php?manual=RNA_Seq_analysis.html)). FPKM from genes expressed in intraradicular
218 mycelium were compared to those of germinating hyphae as a reference. Fold-change
219 values were calculated by proportion-based test statistics (Baggerly et al., 2003) with a
220 False Discovery Rate (FDR) correction for multiple testing (Benjamini et al., 1995). For
221 the present study, we used very stringent parameters and retained only genes showing
222 an expression >5-fold higher in intraradicular mycelium compared to germinating hyphae
223 (FDR \leq 0.05). Among the 26,183 high-confidence genes predicted in *R. irregularis*,
224 17,876 were expressed in hyphae from germinating spores and 12,890 in roots of
225 *B. distachyon*. Among the 31,291 high-confidence genes predicted in *G. rosea*, 13,987
226 genes were expressed in hyphae from germinating spores and 11,896 genes were
227 expressed in roots of *B. distachyon*. The high number of genes expressed in hyphae
228 from germinating spores indicates that this non-symbiotic mycelium was
229 transcriptionally very active and thus, can be used as an appropriate control in
230 transcriptome comparisons. Here, fungal genes showing a higher expression in
231 symbiotic roots compared to germinating hyphae, referred to as symbiosis-related
232 genes. They consist in all genes involved in fungal development and metabolism in
233 plant tissues. These so-called symbiosis-related genes are candidate genes for further
234 functional analyses of symbiotic functions.

235 Detailed information on the protocols and data are available at National Center for
236 Biotechnology Information (NCBI) Gene Expression Omnibus (GEO) portal (accession
237 numbers: GSE67906 to GSE67911 for *G. rosea* and GSE67913 to GSE67926 for
238 *R. irregularis*).

239

240 Protein orthology

241 To assess the orthology between gene sets from the eight species of Mucoromycota
242 sensu Spatafora et al. (2016), we downloaded gene models of *Mortierella elongata* AG-
243 77 v2.0 (Uehling et al., 2017), *Mucor circinelloides* CBS277 v2.0 (Corrochano et al.,
244 2016), *Phycomyces blakesleeanus* NRRL1555 v2.0 (Corrochano et al., 2016) and
245 *Rhizopus microcarpus* ATCC52814 v1.0 (Lastovetsky et al., 2016) from JGI

246 MycoCosm database. We clustered the predicted proteins of these taxa, together with
247 the present Glomeromycotina predicted proteins, with FastOrtho using 50% identity and
248 50% coverage (Wattam et al., 2013). We selected the latter parameters because
249 compared fungal species are highly divergent. We discussed the protein families
250 (orthogroups) in expansion in each species relative to the other species only when the
251 differences were statistically supported (Wattam et al., 2013). Based on this clustering,
252 we determined (1) the set of predicted proteins shared by the eight species (i.e., core
253 genes), (2) sets of predicted proteins encoded in at least two genomes (i.e., dispensable
254 genes), and (3) sets of predicted proteins unique to a genome (i.e., species-specific
255 genes, which are also referred to as taxonomically restricted genes). To define sets of
256 species-specific genes in a broader context, we also searched for orthologous sequences
257 (50% identity and 50% coverage) in a wider set of genomes, ca. all fungal genomes
258 publicly available at MycoCosm. For each gene sets, we also identified duplicated
259 genes. Note that genes families were also automatically clustered by the JGI prediction
260 pipeline and the clusters can be visualized, ranked and compared at the ‘CLUSTERS’
261 page of the JGI Glomeromycotina genome portals, e.g.
262 [https://genome.jgi.doe.gov/clm/run/Rhiir2_1-FM2-Glomeromycota-](https://genome.jgi.doe.gov/clm/run/Rhiir2_1-FM2-Glomeromycota-only.2100;Pe_ufO?organism=Rhiir2_1)
263 [only.2100;Pe_ufO?organism=Rhiir2_1](https://genome.jgi.doe.gov/clm/run/Rhiir2_1-FM2-Glomeromycota-only.2100;Pe_ufO?organism=Rhiir2_1). Multigene families were analysed for
264 statistically significant evolutionary changes in protein family size using the CAFE and
265 FastOrtho programs (Han et al., 2013; Wattam et al., 2013) with default parameters.
266 The genomes of *R. clarus* (Kobayashi et al., 2018) and *D. epigaea* (Sun et al., 2018)
267 were not included in these analyses, as they were publicly released after this manuscript
268 submission.

269

270 Phylogenomic analysis

271 A phylogenomic tree was constructed using the eight above mentioned Mucoromycota
272 genomes and four outgroup genomes. We identified 784 gene clusters with only one
273 protein-coding gene per species by clustering protein sequences using FastOrtho
274 (Wattam et al., 2013) with the following parameters: 50% identity and 50% coverage.
275 Each cluster was then aligned with MAFFT 7.221 (Katoh & Standley, 2002), and
276 ambiguous regions (containing gaps and poorly aligned) were eliminated and single-
277 gene alignments were concatenated with GBLOCKS 0.91b (Castresana, 2000). A

278 maximum likelihood inference for our phylogenomic dataset was achieved with
279 RAxML 7.7.2 (Stamatakis, 2014) using the standard algorithm, the
280 PROTGAMMAWAG model of sequence evolution and 1000 bootstrap replicates.
281
282 dN/dS calculation
283 For this analysis, we only used gene nucleotide sequences defined as 1-1-1-1-1
284 orthologues by FastOrtho. Average dN and dS values for predicted transcripts were
285 calculated using the BioPerl's DNAStatistics package (Stajich et al., 2002). The
286 package uses a simple count method for dN and dS calculations, which is sufficient for
287 our purposes of finding divergent orthogroups in the clusters as defined above.
288 Alignments were confirmed by visual inspection. To ensure a conserved analysis,
289 poorly aligned loci were discarded from the average dN and dS analysis and the final
290 results were plotted using the R program. A list of the genes showing evidence of rapid
291 sequence evolution in the Glomeromycotina genomes and their putative function (KOG
292 definition) can be found in the Supporting Information.
293
294 Single nucleotide polymorphism (SNP)
295 For SNP calling and allelic frequencies plots, each set of paired-end and mate-pair data
296 sets used for Glomeromycotina assemblies was mapped independently against the
297 respective corresponding reference genome assemblies downloaded from the JGI
298 portals using the Burrows–Wheeler Alignment (BWA) tool, with the BWA-MEM
299 algorithm (Li & Durbin, 2009). The mapping tool is specifically designed for sequences
300 ranging from 70 bp to 1 Mbp and is recommended for high-quality queries. SAMtools
301 (Li et al., 2009) was then used to convert SAM files into sorted BAM files and to merge
302 the different data sets of the same species together, to obtain a single sorted BAM file
303 for each isolate. SNPs were called using FreeBayes v0.9.18-3-gb72a21b (Garrison &
304 Marth, 2012), with the following parameters: -K (that is, output all alleles that pass
305 input filters), excluding alignments with mapping quality less than 20 (-m 20) and
306 taking into account only SNPs with at least two alternate reads (-C 2). SNPs were
307 filtered to avoid the analysis of false positives (that is, SNPs originating from
308 misalignment and/or paralogy) using vcf-filter from the vcf-lib library according to (1)
309 the read depth (maximum read depth: $DP < 1.25 \times$ genome mean coverage; minimum

310 read depth: $DP > 0.75 \times$ genome mean coverage), (2) the type of SNPs (only considering
311 SNPs, not indels: TYPE = snp), (3) considering only one alternative allele (NUMALT =
312 1) and (4) the reference allele observation ($RO > 1$).

313

314 Data availability

315 Full genome, predicted gene and transcript sequences of *R. irregularis* DAOM197198,

316 *R. diaphanus* MUCL 43196, *R. cerebriforme* DAOM 227022 and *G. rosea*

317 DAOM194757 can be accessed at:

318 https://genome.jgi.doe.gov/Rhiir2_1/Rhiir2_1.home.html;

319 <https://genome.jgi.doe.gov/Rhidi1/Rhidi1.home.html>;

320 https://genome.jgi.doe.gov/Rhice1_1/Rhice1_1.home.html;

321 <https://genome.jgi.doe.gov/Gigro1/Gigro1.home.html>.

322 Genomic resources are also available at GenBank under the following accession

323 numbers: *R. irregularis* DAOM197198 version 2, AUPC02000000/PRJNA208392;

324 *R. diaphanus*, QKKE01000000/PRJNA430014; *R. cerebriforme*,

325 QKYT01000000/PRJNA430010; and *G. rosea*, QKWP01000000/PRJNA430513.

326

327 **Results**

328 General genome features and phylogeny

329 The nuclear genomes of *R. irregularis*, *R. diaphanus* and *R. cerebriforme* in Glomerales

330 and *Gigaspora rosea* in Diversiporales were sequenced and assembled. They ranged

331 from 126 to 598 Mbp with an estimated content of 21,549 to 31,291 protein-coding

332 genes (Table 1, Supplementary Table S1 in Supporting Information). Glomeromycotina

333 genomes are significantly larger than saprotrophic Mucoromycota genomes (Table 1).

334 No evidence of whole genome duplication events (i.e., no segmental duplications) was

335 found (see Synteny tools on the JGI portals) and this larger size is mainly driven by TE

336 proliferation. TE content ranges from 20% (*R. diaphanus*) to 63% (*G. rosea*) of total

337 assemblies (Table 1, Fig. 1). However, the exact repetitive fraction of *G. rosea* and

338 *Rhizophagus* genomes is likely larger; their highly repetitive nature (Fig. 1) has

339 contributed to the assembly fragmentation, hindering the annotation of an unknown TE

340 proportion. The distribution of TE categories notably varies between *G. rosea* and

341 *Rhizophagus* spp. (Fig. 1), with the former harbouring a larger genome coverage of

342 Gypsy LTR, Tad1, hAT and Mariner/Tc1. The number of Penelope retroelement copies
343 in *G. rosea* is >3,900, whereas only 206 copies are found in *R. cerebriforme* and none in
344 *R. irregularis* and *R. diaphanus*, indicating that invasions by different types of TE took
345 place independently in different AM fungi. There are hints of older TE propagation
346 events in the four genomes with a long tail of low similarity TE copies (data not
347 shown). As a result of massive TE proliferations, Glomeromycotina genomes show a
348 very high level of structural rearrangements and a macrosynteny was only observed
349 between *R. irregularis* and *R. diaphanus* (Supplementary Fig. S1), consistent with their
350 close phylogenetic proximity.

351 Over 97% of a benchmark set of conserved fungal BUSCO genes, a proxy to genome
352 completeness (Simão et al., 2015), were found in Glomeromycotina assemblies
353 (Supplementary Table S2) and up to 94% of RNA-Seq reads from fungal libraries
354 mapped to the gene repertoire (see Info page on JGI genome portals), indicating that
355 assembled genomes capture most of the coding gene space.

356 To have a robust phylogenetic framework for our comparative analyses, we
357 investigated phylogenetic relationships between the sequenced Glomeromycotina and
358 other Mucoromycota. A phylogeny based on a concatenation of 784 single copy,
359 orthologous protein sequences (Fig. 2) strongly supports the erection of Mucoromycota
360 to unite Glomeromycotina, Mortierellomycotina and Mucoromycotina (Spatafora et al.,
361 2016; Uehing et al., 2017).

362

363 Glomeromycotina-specific gene families: gains and losses

364 We compared the gene repertoires encoded by sampled Mucoromycota taxa and
365 identified sub-phylum- and species-specific gene families that might contribute to
366 genome trait diversification. We separately clustered predicted protein sequences of
367 either the four species of Glomeromycotina or the eight species of Mucoromycota to
368 infer orthologous gene groups (orthogroups) (Wattam et al., 2013). We then identified
369 (i) sets of core genes shared by all Mucoromycota or all Glomeromycotina species; (ii)
370 sets of dispensable genes shared by at least two species of Mucoromycota or
371 Glomeromycotina; (iii) sets of species-specific genes only found in a single genome
372 (Fig. 3, Supplementary Table S3). For each category, we also identified single copy and
373 duplicated genes. As expected for species that diverged >450 million years ago

374 (Uehling et al., 2017), clustering the predicted protein sequences of the eight
375 Mucoromycota led to a very restricted core set of genes (Fig. 3, Supplementary
376 Table S3). In the other hand, we identified 5,463 to 5,703 conserved (core) genes, 24 to
377 27% of them being duplicated genes, in Glomeromycotina species (Supplementary
378 Table S3). Each AM species is characterized by a large set of species-specific genes,
379 which are also referred to as taxonomically restricted genes. Within this context, the
380 very high proportion of species-specific-genes in *G. rosea* (64%) with a higher
381 frequency of multi-allelic copy numbers (Fig. 3, Supplementary Table S3) is intriguing
382 and partly reflects the large taxonomic divergence between this taxon and those
383 sequenced so far. These sets of Glomeromycotina species-specific genes are noticeably
384 distinct as they have a shorter gene size, fewer exons, and a lower proportion of
385 expressed sequences than the conserved genes (Supplementary Table S4), suggesting
386 they might be evolutionarily young genes.

387 The expansion and contraction of gene families (i.e., orthogroups) in the different
388 lineages of Mucoromycota were determined by using the gene family modeling pipeline
389 CAFE (Han et al., 2013) (Supplementary Fig. S2) and FastOrtho (Supplementary
390 Tables S5 to S8). Across the phylogeny, the number of orthologous gene families
391 gained on Glomeromycotina and Mucoromycotina lineages, relative to their most recent
392 common ancestor (MRCA), are in the same range, from 63 to 259 (<10% of the
393 orthologous protein sets). Gene family loss was also rampant during the diversification
394 throughout the Mucoromycota lineages and is larger in *G. rosea*.

395 It is noteworthy that several Glomeromycotina gene families are strikingly expanded
396 (i.e., they contain a larger set of duplicated genes) or not shared with Mucoromycotina
397 or *M. elongata* (duplicated species-specific genes in Fig. 3, Supplementary Tables S5 to
398 S8). They include large gene families encoding protein domains related to signaling
399 kinases, such as tyrosine kinase specific for activated GTP (p21cdc42Hs) and
400 ubiquitination-associated BTB/POZ domain-containing proteins (Supplementary Table
401 S9). Tyrosine kinases are often associated to Sell repeats which can serve as adaptor
402 proteins for the assembly of macromolecular complexes under cellular stress (Mittl and
403 Schneider-Brachert, 2007).

404 Hierarchical clustering of the presence and abundance of the different Pfam protein
405 domains found in the genomes of Mucoromycota species (this study) and *R. irregularis*

406 isolates (Chen et al., 2018) (Fig. 4A) identified genome-wide patterns of functional
407 domain content among these fungi. Glomeromycotina clustered together, whereas
408 Mucoromycotina species clustered with *M. elongata*. Among Glomerales, *R. diaphanus*
409 was closely related to the five sequenced *R. irregularis* isolates, whereas
410 *R. cerebriforme* displays a substantial divergence in its Pfam domain distribution.
411 Although clustering with Glomerales, *G. rosea* displayed a Pfam domain distribution
412 pattern very different from these species, pointing to large differences in metabolic,
413 developmental and signalling pathways between AM fungi. Pfam categories showing a
414 substantial differential abundance contain genes encoding transcriptional factors, e.g.
415 Myb proteins and DNA polymerase, but also key factors involved in cell structure, such
416 as adaptins and kinesins. In *Rhizophagus* spp., the distribution of Pfam domains
417 corroborated the higher occurrence of proteins predicted to have a role in signaling
418 pathways and protein-protein interactions (see above, Tables S5, S6, S7 and S9). The
419 *G. rosea* gene set is enriched in AMP-binding and tetratricopeptide repeat region
420 (TPR)-domain containing proteins, H⁺-ATPases, NUDIX hydrolases, aspartyl proteases,
421 cytochromes P450, and methyltransferases (Fig. 4A).

422 The functional genomic comparison made through KEGG pathway profile
423 correlations (Fig. 4B) also showed that sequenced Glomeromycotina present a higher
424 metabolic similarity between taxa compared to *M. elongata*/Mucoromycota species,
425 corroborating and extending *M. elongata* genome analysis (Uehling et al., 2017). Lack
426 of PCWDE (see below), degradation of sucrose and glycogen (i.e. invertase,
427 glucoinvertase, glucoamylase), biosynthesis of polyketides, nonribosomal peptides,
428 thiamin and biosynthesis of fatty acids (i.e. palmitic acid through type I fatty acid
429 synthase) are among the most noticeable metabolic idiosyncrasies of Glomeromycotina
430 (see KEGG comparative tool on JGI portals).

431 A substantial proportion (44 to 47%) of predicted Glomeromycotina genes have no
432 sequence similarity with documented proteins in MycoCosm (Fig. 3), Pfam
433 (Supplementary Table S1) or Eukaryotic Orthologous Groups of Proteins (KOG)
434 databases (data not shown).

435 Nucleotide sequences of Glomeromycotina orthologous genes (1-1-1-1-1) were
436 aligned to identify any evidence of accelerated sequence evolution, assuming that
437 increased sequence divergence results from positive selection, possibly caused by

438 environmental pressures (Supplementary Fig. S3). The analysis revealed that most of
439 the 100 orthologous genes showing the highest sequence divergence (i.e. red dots in
440 Supplementary Fig. S3) encode for proteins with unknown function (Supplementary
441 Table S10). Orthologues with putative function are involved in a large variety of
442 biologically unrelated functions and pathways and, for example, include HMG-box
443 transcription factors, RNA polymerases, as well as protein required for meiotic
444 chromosome segregation (KOG2513), or mitochondrial Fe/S cluster exporters.

445

446 A restricted set of genes involved in lignin and polysaccharide degradation

447 The sequenced Glomeromycotina species share a limited repertoire of genes coding for
448 secreted plant cell wall degrading enzymes (PCWDE) (Fig. 5, Supplementary Fig. S4,
449 Supplementary Table S11). No gene encoding lignin peroxidases (AA2),
450 cellobiohydrolases (GH6, GH7), polysaccharide lyases (PL1, PL3, PL4, PL9), lytic
451 polysaccharide monooxygenases acting on cellulose or cellulose-binding-,
452 carbohydrate-binding module 1 (CBM1) are encoded by sequenced Glomeromycotina
453 genomes. In *Rhizophagus* spp., only a single endo- β -1,4-endomannanase (GH5_27) is
454 possibly acting on hemicellulose in plant cell walls. The secreted polysaccharidases
455 annotated in *Rhizophagus* species are mostly acting on fungal polysaccharides
456 (chitooligosaccharide oxidase AA7, chitin deacetylase CE4, chitinase GH18 and α -N-
457 acetylgalactosaminidase GH27) or bacterial peptidoglycans (lysozyme GH25) (Fig. 5,
458 Supplementary Fig. S4, Supplementary Table S11). The only carbohydrate-binding
459 modules are chitin-binding modules (CBM18, CBM19). Remarkably, the distribution of
460 several CAZyme families strikingly differ in *G. rosea* compared to *Rhizophagus*
461 species, i.e., higher copy number of laccase (AA1) possibly acting on polyphenolic
462 compounds, cellobiose dehydrogenase AA3, chitooligosaccharide oxidase AA7,
463 chitinases GH18, α -N-acetylgalactosaminidase GH27, mannosyl-oligosaccharide α -1,2-
464 mannosidase GH92, galactoside α -1,3/1,4-L-fucosyltransferase GT10,
465 lipopolysaccharide β -1,4-galactosyltransferase GT25 and carbohydrate-binding modules
466 binding to chitin (CBM14, CBM18) in *G. rosea* (Fig. 5, Supplementary Fig. S4,
467 Supplementary Table S11).

468

469 Sexual reproduction

470 The Glomeromycotina genomes were also investigated for the presence of genomic
471 signatures of sexual reproduction (Riley et al. 2013), particularly meiosis-specific genes
472 (MSG), and for evidence of a homokaryotic/dikaryotic genetic organization; the latter
473 being defined by the co-existence of one or two divergent putative mating-type MAT
474 loci, as recently found in some *R. irregularis* isolates (Ropars et al., 2016). Our
475 analyses are consistent with recent data based on analyses of *R. irregularis* assemblies
476 (Ropars et al., 2016, Chen et al., 2018), as we found that all genomes encode for a
477 complete set of MSG (Supplementary Table S12A). Furthermore, all AM fungi in this
478 study show intra-isolate genetic variation (0.23 to 0.36 SNP per kb) (Supplementary
479 Table S12B) that are consistent with a homokaryotic genome organization with no
480 evidence of dikaryosis. The distribution of DNA reads mapping on all bi-allelic SNP
481 regions were assessed and we observed allele frequencies in agreement with haploid
482 genome patterns (Supplementary Fig. S5).

483 Also consistent with the homokaryotic nature of these species, each one carried a
484 single copy of a genomic region showing similarities with a MAT locus composed of
485 two bi-directionally transcribed genes with homeodomain regions, with coiled-coil
486 domains and nuclear localization signals. We took advantage of the newly available
487 genome data to determine whether the locus is structurally conserved across the AM
488 fungal phylogeny, an indication that conservation in gene order is functionally
489 important for the locus. Our analyses showed that the putative AM fungal MAT-locus is
490 conserved in structure across most Glomeromycotina species investigated to date with
491 the exception of *G. rosea*, including the basal genera *Claroideoglosum* and *Paraglosum*
492 (Supplementary Fig. S6). It also shows substantial sequence divergence among the
493 species investigated, as expected for bone-fide MAT-loci. The absence of structural
494 conservation of HD-1-like and HD-2 genes in Gigasporaceae stands out, particularly
495 given that the locus is conserved in other members of the Diversisporaceae; namely *D.*
496 *epigaea*.

497
498 Secretome and candidate effectors in Glomeromycotina

499 *G. rosea* and *M. elongata* have the largest repertoire of secreted proteins, whereas other
500 species have similar sets of secreted proteins, such as CAZymes, proteases and lipases

501 (Supplementary Table S13). *R. irregularis* presents a larger repertoire of small secreted
502 proteins (SSP) compared to other Glomales. Among 436 orthogroups coding for SSPs,
503 250 are specific to Glomeromycotina species, while 45 are specific to *G. rosea* and 138
504 only represented in Rhizophagus species (Supplementary Table S14), confirming that
505 AM fungi have substantial species-specific repertoire of SSPs.

506

507 Conservation of symbiosis-related transcriptional signature within Glomeromycotina
508 The expression of *R. irregularis* genes was measured by RNA-Seq profiling in
509 *B. distachyon mycorrhizae*; 426 *R. irregularis* transcripts (3.3% of the expressed genes)
510 are expressed at a higher level in symbiotic roots compared to transcriptionally-active
511 germinating hyphae (Supplementary Table S15A). These transcripts are potentially
512 involved in the development and physiology of the symbiotic interaction. We assessed
513 the evolutionary conservation of these symbiosis-related transcripts among
514 Mucoromycota (Fig. 6A). We found that only 16 % of *R. irregularis* symbiosis-
515 upregulated genes are shared by all species of Mucoromycota (cluster VIII). Most of
516 them are coding for core metabolic functions. In addition, most transcripts from cluster
517 IV have orthologous sequences in Glomeromycotina and one or several species of
518 saprotrophic Mucoromycota. On the other hand, only seven % of *R. irregularis*
519 symbiosis-induced genes are species-specific (cluster VII), i.e. not even shared with its
520 closest taxa, *R. diaphanus*. Most of these genes code for proteins with unknown KOG
521 functions and mycorrhiza-induced small secreted proteins (MiSSPs). Cluster II (8%)
522 grouped *R. irregularis* symbiosis-induced genes, mainly coding for unknown proteins
523 and MiSSPs, having a strong similarity with *R. diaphanus*, its closest relative.
524 Transcripts of clusters III and V (36%) are shared by the Glomeromycotina species,
525 while those of cluster VI (7%) are only encoded by *G. rosea* and *R. cerebriforme*. As
526 expected, sequence conservation reflects the phylogenetic distance between taxa, e.g.,
527 80 % of *R. irregularis* symbiosis-induced genes are found in *R. diaphanus* with a high
528 sequence similarity (> 80 %). A substantial proportion of these Glomeromycotina-
529 conserved, symbiosis-related genes have no known function. However, among genes
530 conserved in *G. rosea* and Rhizophagus species (clusters III, IV, V and VIII), several
531 are involved in primary metabolism, e.g. nitrogen and carbon assimilation, membrane
532 transport, signaling pathways (Supplementary Table S15A). Genes putatively involved

533 in detoxification mechanisms are also widely represented, e.g. cytochrome P450, UDP-
534 glucuronosyl transferase, glutathione-S-transferase and pleiotropic drug resistance
535 proteins (PDR1-15).

536 Analysis of the differential gene expression during the *G. rosea*/B. distachyon
537 interaction identified 989 *G. rosea* genes (8.3% of the expressed genes) having a higher
538 expression in symbiotic tissues compared to germinating hyphæ (Supplementary
539 Table S15B). We investigated the evolutionary conservation of these transcripts
540 enriched in symbiotic tissues among Mucoromycota (Fig. 6B). Intriguingly, a larger
541 proportion (48%, clusters V, VI and VII) of symbiosis-related *G. rosea* genes are
542 conserved in the eight Mucoromycota species compared to *R. irregularis*. Most of them
543 are involved in cellular and signaling processes, and metabolism. Fourteen % of
544 symbiosis-upregulated genes (cluster IV) are specific to *G. rosea*, coding for proteins of
545 unknown KOG function and MiSSPs (Fig. 6B, Supplementary Table S15B). Similarly,
546 *G. rosea* symbiosis-upregulated genes shared with Rhizophagus species (cluster II) are
547 coding for proteins of unknown KOG function and MiSSPs.

548

549 **Discussion**

550 In the present study, we investigated the evolutionary dynamics of key genomic traits in
551 the subphylum Glomeromycotina of Mucoromycota (Spatafora et al., 2016). Our
552 enhanced AM fungal taxon sampling, including three newly annotated genomes
553 (*R. diaphanus*, *R. cerebriforme*, *G. rosea*) and an improved *R. irregularis*
554 DAOM197198 assembly and annotation (Chen et al., 2018), allows us to perform both
555 within- and across-lineage comparisons, thus covering the different time scales at which
556 the evolution of genome features occurred. In addition, this comparative genomic study
557 provides further insights on the gene repertoires of AM fungi. Overall, our findings
558 show that extant Glomeromycotina genomes have been shaped by both retention of
559 ancestral states present in saprotrophic Mucoromycota and secondary innovations, for
560 the multiple genomic traits investigated in the present study, namely genome size,
561 protein domain diversity and gene content.

562 Genomic features (e.g. genome size, gene number, TE content) are highly similar
563 within Glomerales. In contrast, *G. rosea* genome is much larger (>600 Mb) with a
564 larger coding space and higher TE content. Previously, our knowledge on AM fungal

565 genomics was limited to the genus *Rhizophagus*, mainly the model fungus *R. irregularis*
566 (Tisserant et al., 2013; Li et al., 2014; Ropars et al., 2016; Chen et al., 2018; Maeda et
567 al., 2018). Although the transcriptome of *G. rosea* (Tang et al., 2016) and *G. margarita*
568 (Salvioli et al., 2016) have been sequenced, the genome of these representatives of the
569 Diversiporales was not sequenced. Therefore, the present study improves our
570 knowledge on genomics and evolutionary biology of AM fungi by including genome
571 information on *G. rosea*.

572 Our findings reveal a remarkable convergence in genome evolution in Glomerales
573 and Diversiporales with massive accumulation of TE, extensive gene duplications in
574 species-specific families and signaling pathways, but also losses of genes related to
575 saprotrophism in Mucoromycota. We identified large sets of Glomeromycotina-specific
576 genes by comparing Mucoromycota genomes, though most of them are coding for
577 proteins with unknown function, such as MiSSPs. Gene families in expansion that
578 originated in lineages leading to extant AM fungal species and genes specific to the
579 Glomeromycotina subphylum are thought to operate in pathways or developmental
580 processes, e.g. symbiotic interactions, that distinguish AM fungi from other
581 Mucoromycota. Confirmation of this contention will require further large scale
582 functional analyses.

583 We also showed the consistent lack of enzymes involved in plant cell wall
584 degradation, thiamin biosynthesis, and cytosolic fatty acid synthesis in the four
585 Glomeromycotina genomes, the consistent presence of genes involved in sexual
586 reproduction in the four genomes, genus-specific sets of small secreted proteins that
587 may play a role in symbiont recognition and accommodation. A low proportion (16%) of
588 genes upregulated in symbiotic tissues are conserved in Mucoromycotina genomes.
589 Those conserved genes mainly encode for cellular and signaling processes, and
590 pathways of the primary metabolism, and likely derived from those encoded by the
591 saprotrophic MRCA. Several of these general genomic features have recently been
592 confirmed in *G. clarus* (Kobayashi et al., 2018) and *D. epigaea* (Sun et al., 2018).

593 The very large sets of species-specific genes found in each clade of
594 Glomeromycotina suggest that de novo gene construction followed by extensive gene
595 duplications, and/or fast sequence evolution of pre-existing genes is a hallmark of the
596 sampled AM fungal genomes. As these species-specific genes have no ortholog in other

597 sequenced taxa, they evolved independently in each AM species, i.e. they are not
598 derived from ancestral saprotrophic Mucoromycota. This is particularly true for
599 *G. rosea* which displays the largest gene repertoire of sequenced AM fungi so far.
600 Several of these expanding gene families are coding for symbiosis-upregulated orphan
601 genes, that are possibly playing a role in symbiosis. For example, we found dozens of
602 MiSSPs in each taxa of AM fungi that may code for candidate effector proteins. It
603 remains to investigate whether they play a role in host specificity and in symbiosis
604 development as suggested by Kamel et al. (2017) and Zeng et al. (2018). Maeda et al.
605 (2018) showed that TE contribute to gene duplication in several gene families in
606 *R. irregularis*. Investigating the role of TE in the massive gene duplications observed in
607 *G. rosea* will require a genome assembly of higher quality. The present study confirms
608 and extends our initial findings (Tisserant et al., 2013) that protein kinase genes, such as
609 those coding for protein tyrosine kinases, are among the largest gene families identified
610 in AM fungal taxa. It is tempting to speculate that this large number of protein sensors
611 play a role in symbiotic interactions, such as host specificity, and in planta
612 accomodation of AM fungi.

613 Selected species in the Mucoromycotina sub-phylum includes fast growing, early
614 colonizers of carbon-rich substrates such as *Mucor* and *Rhizopus*. They possess a
615 substantial number of lignocellulose-degrading enzymes, although their set of PCWDE,
616 especially those targeting crystalline cellulose (e.g., GH6, GH7, AA9 and CBM1)
617 (Fig. 5, Supplementary Fig. S4), is lower than wood decayers in Dikarya (Kohler et al.,
618 2015; Uehling et al., 2017). As obligate biotrophs, AM fungi do not need a repertoire of
619 polysaccharide degrading enzymes because they derive most (if not all) of their carbon
620 from their hosts, but the complete lack of genes acting on plant cell wall
621 polysaccharides in *Rhizophagus* species is intriguing and gives rise to the question of
622 how hyphae colonize the apoplastic space of host roots and how they degrade host cell
623 walls to colonize host cells. The few remaining enzymes, i.e., multicopper oxidases
624 (AA1), endoglucanase GH5_7, xyloglucanase GH5_12 and xyloglucosyltransferase
625 GH16, are prime candidates for further functional analysis of fungal colonisation in
626 planta. In addition to the loss of their saprotrophic enzymatic arsenal, AM fungi are
627 lacking genes needed for thiamine biosynthesis, secondary metabolites and cytoplasmic
628 fatty acid synthesis. This reduction in the biosynthetic ability is also observed in several

629 obligate biotrophic pathogens (Spanu, 2012). The evolutionary mechanism behind this
630 convergent gene loss is not known, but it is supporting the assumption that their
631 function has become obsolete due to the obligate biotrophic lifestyle.

632 The analysis of the present AM fungal genomes, together with the recently published
633 *R. clarus* (Kobayashi et al., 2018) and *D. epigaea* (Sun et al., 2018) genomes,
634 confirmed that AM fungal genomes are haploid and their genomic polymorphism is
635 very low (0.14 to 0.35 SNP per kb). It also confirmed the presence of the gene
636 machinery usually related to sex (e.g., MSG and putative MAT-loci) in these putative
637 asexual clonal lineages. These genes are likely involved in the recently observed inter-
638 nuclear recombination taking place in the dikaryotic life-stage of the *R. irregularis*
639 isolates A4 and A5 (Chen et al., 2018b).

640 Obviously, we cannot sequence the genome of the unknown MRCA of
641 Glomeromycotina and Mucoromycotina to identify the gene set involved in the
642 transition from saprotrophism to symbiosis and obligate mutualism. Sequencing
643 genomes of a much larger and diverse set of Mucoromycota associated to early land
644 plants and of fine root endophytes (Field & Pressel, 2018) may facilitate the
645 reconstruction of the genome of these ancient species which gave rise to the symbiotic
646 lineage(s). Although Endogonales and Glomeromycotina are not sister groups and
647 represent independent origins of mycorrhizal lifestyle within Mucoromycota, it is worth
648 mentioning that the most prominent genome features of ectomycorrhizal Endogonaceae
649 is their high TE content and a reduced number of PCWDE (Chang et al., 2018).

650 In conclusion, the present genome comparison refines our understanding of what
651 makes Glomeromycotina unique. Their genomic features have arisen repeatedly in
652 several independent lineages, likely as a result of convergence of evolutionary traits,
653 suggesting that such adaptations can be favoured by selection. It is not yet known
654 whether the identified genomic features are shared by the 315 AM fungal species.
655 Despite the global dominance of Glomerales over the other AM fungal families, it is
656 crucial to further corroborate our findings with improved sampling of other taxa from
657 the more ancient, non-Glomerales families, such as Archeosporales and Paraglomerales.
658

659 **Acknowledgements**

660 We would like to thank Annegret Kohler, Claude Murat, Alexandre Poliakov, Christine
661 Strullu-Derrien and Joseph Spatafora for discussions and advices. FMM's work is
662 funded by the Laboratory of Excellence ARBRE (ANR-11-LABX-0002-01), Region
663 Lorraine, European Regional Development Fund and Beijing Advanced Innovation
664 Center for Tree Breeding by Molecular Design, Beijing Forest University. NC's work is
665 supported by the Discovery program from Natural Sciences and Engineering Research
666 Council of Canada (NSERC-Discovery), an Early Researcher Award from Ontario
667 Ministry of Research and Innovation (ER13-09-190) and ZygoLife project funded by
668 the U.S. National Science Foundation (DEB 1441677). CR is funded by the Laboratory
669 of Excellence TULIP (ANR-10-LABX-41). Genome annotations were performed using
670 the annotation pipeline of the U.S. DOE JGI (Contract DE-AC02-05CH11231) (1000
671 Fungal Genomes project and Mycorrhizal Genomics Initiative).

672
673 **Author contributions**

674 F.M.M., C.R. and N.C. planned and designed the research, wrote the manuscript, and
675 helped with data analysis. E.M., H.S.C., E.C.H.C., S.M., A.P., I.D.L.P, M.H., E.D., and
676 B.H. performed bioinformatic analyses; E.M. and N.T. performed the transcriptome
677 analyses. A.K. and I.V.G. supervised the JGI gene prediction pipeline. S.R. and J.V.
678 produced the biological material. I.D.L.P., S.N., D.B. produced DNA material and DNA
679 sequences. CR and FMM were joint senior authors on this work.

680
681 **References**

- 682 **Altschul SF, Gish W, Miller W, Myers EW, Lipman DJ. 1990.** Basic local alignment
683 search tool. *Journal of Molecular Biology* **215**: 403–410.
- 684 **Baggerly KA., Deng L, Morris JS, Aldaz CM. 2003.** Differential expression in
685 SAGE: accounting for normal between-library variation. *Bioinformatics* **19**: 1477-
686 1483.
- 687 **Beaudet D, Chen ECH, Mathieu S, Yildirim G, Ndikumana S, Dalpé Y, Séguin S,**
688 **Farinelli L, Stajich JE, Corradi N. 2018.** Ultra-low input transcriptomics reveal the
689 spore functional content and phylogenetic affiliations of poorly studied arbuscular
690 mycorrhizal fungi. *DNA Research*: **25**: 217-227.

691 **Bécard G, Fortin JA. 1988.** Early events of vesicular arbuscular mycorrhiza formation
692 on Ri T-DNA transformed roots. *New Phytologist* **108**: 211–218.

693 **Benjamini Y, Hochberg Y. 1995.** Controlling the false discovery rate - a practical and
694 powerful approach to multiple testing. *Journal of the Royal Statistical Society, Series*
695 *B, Statistical Methodology* **57**: 289–300.

696 **Bolger AM, Lohse M, Usadel B. 2014.** Trimmomatic: a flexible trimmer for Illumina
697 sequence data. *Bioinformatics* **30**: 2114–20.

698 **Bonfante P, Genre A. 2008.** Plants and arbuscular mycorrhizal fungi: an evolutionary-
699 developmental perspective. *Trends in Plant Science* **13**: 492–498.

700 **Bravo A, Brands M, Wewer V, Dörmann P, Harrison MJ. 2017.** Arbuscular
701 mycorrhiza-specific enzymes FatM and RAM2 fine-tune lipid biosynthesis to
702 promote development of arbuscular mycorrhiza. *New Phytologist* **214**: 1631–1645.

703 **Brundrett MC, Tedersoo L. 2018.** Evolutionary history of mycorrhizal symbioses and
704 global host plant diversity. *New Phytologist* **220**: 1108–1115.

705 **Bruns TD, Corradi N, Redecker D, Taylor JW, Öpik M. 2018.** Glomeromycotina:
706 what is a species and why should we care? *New Phytologist* **220**: 963–967.

707 **Castresana J. 2000.** Selection of conserved blocks from multiple alignments for their
708 use in phylogenetic analysis. *Molecular Biology and Evolution* **17**: 540–552.

709 **Chang Y, Wang S, Sekimoto S, Aerts AL, Choi C, Clum A, LaButti KM, Lindquist**
710 **EA, Yee Ngan C, Ohm RA et al. 2015.** Phylogenomic analyses indicate that early
711 Fungi evolved digesting cell walls of algal ancestors of land plants. *Genome Biology*
712 *and Evolution* **7**: 1590–1601.

713 **Chang Y, Desirò A, Na H, Sandor L, Lipzen A, Clum A, Barry K, Grigoriev IV,**
714 **Martin FM, Stajich JE, Smith ME, Bonito G, Spatafora JW. 2018.**
715 Phylogenomics of Endogonaceae and evolution of mycorrhizae within
716 Mucoromycota. *New Phytologist*. doi.org/10.1111/nph.15613.

717 **Chen ECH, Morin E, Beaudet D, Noel J, Yildirim G, Ndikumana S, Charron P,**
718 **St-Onge C, Giorgi J, Krüger M et al. 2018a.** High intraspecific genome diversity in
719 the model arbuscular mycorrhizal symbiont *Rhizophagus irregularis*. *New*
720 *Phytologist* **220**: 1161–1171.

721 **Chen ECH, Mathieu S, Hoffrichter A, Sedzielewska-Toro K, Peart M, Pelin A,**
722 **Ndikumana S, Ropars J, Dreissig S, Fuchs J, Brachmann A, Corradi N. 2018b.**
723 Single nucleus sequencing reveals evidence of inter-nucleus recombination in
724 arbuscular mycorrhizal fungi. *eLife* **7**: e39813.

725 **Corradi N, Brachmann A. 2017.** Fungal mating in the most widespread plant
726 symbionts? *Trends in Plant Science* **22**: 175–183.

727 **Corrochano LM, Kuo A, Marcet-Houben M, Polaino S, Salamov A, Villalobos-**
728 **Escobedo JM, Grimwood J, Álvarez MI, Avalos J, Bauer D et al. 2016.**
729 Expansion of signal transduction pathways in fungi by extensive genome
730 duplication. *Current Biology* **26**: 1577-1584.

731 **Coupe SA, Deikman, J. 1997.** Characterization of a DNA-binding protein that interacts
732 with 5' flanking regions of two fruit-ripening genes. *Plant Journal* **11**: 1207-1218.

733 **Field KJ, Pressel S. 2018.** Unity in diversity: structural and functional insights into the
734 ancient partnerships between plants and fungi. *New Phytologist* **220**: 996–1011.

735 **Garrison E, Marth G. 2012.** Haplotype-based variant detection from short-read
736 sequencing. arXiv preprint: 1207.3907 [q-bio.GN]

737 **Gnerre S, MacCallum I, Przybylski D, Ribeiro FJ, Burton JN, Walker BJ, Sharpe**
738 **T, Hall G, Shea TP, Sykes S et al. 2011.** High-quality draft assemblies of
739 mammalian genomes from massively parallel sequence data. *Proceedings of the*
740 *National Academy of Sciences* **108**: 1513–1518.

741 **Grigoriev IV, Nikitin R, Haridas S, Kuo A, Ohm R, Otilar R, Riley R, Salamov A,**
742 **Zhao X, Korzeniewski F et al. 2014.** MycoCosm portal: gearing up for 1000 fungal
743 genomes. *Nucleic Acids Research* **42**: D699–D704

744 **Han MV, Thomas GW, Lugo-Martinez J, Hahn MW. 2013.** Estimating gene gain and
745 loss rates in the presence of error in genome assembly and annotation using CAFE 3.
746 *Molecular Biology and Evolution* **30**: 1987-1997.

747 **Idnurm A, Hood ME, Johannesson H, Giraud T. 2015.** Contrasted patterns in
748 mating-type chromosomes in fungi: Hotspots versus coldspots of recombination.
749 *Fungal Biology Reviews* **29**: 220–229.

750 **Kamel L, Tang N, Malbreil M, San Clemente H, Le Marquer M, Roux C, Frei dit**
751 **Frey N. 2017.** The comparison of expressed candidate secreted proteins from two

752 arbuscular mycorrhizal fungi unravels common and specific molecular tools to
753 invade different host plants. *Frontiers in Plant Science* **8**: 124

754 **Katoh K, Standley DM. 2013.** MAFFT Multiple Sequence Alignment Software
755 Version 7: Improvements in Performance and Usability. *Molecular Biology and*
756 *Evolution* **30**: 772-780.

757 **Kobayashi Y, Maeda T, Yamaguchi K, Kameoka H, Tanaka S, Ezawa T,**
758 **Shigenobu S, Kawaguchi M. 2018.** The genome of *Rhizophagus clarus* HR1
759 reveals a common genetic basis for auxotrophy among arbuscular mycorrhizal fungi.
760 *BMC Genomics* **19**: 465.

761 **Krüger M, Krüger C, Walker C, Stockinger H, Schüssler A. 2012.** Phylogenetic
762 reference data for systematics and phylotaxonomy of arbuscular mycorrhizal fungi
763 from phylum to species level. *New Phytologist* **193**: 970-984.

764 **Lanfranco L, Fiorilli V, Gutjahr C. 2018.** Partner communication and role of
765 nutrients in the arbuscular mycorrhizal symbiosis. *New Phytologist* **220**: 1031–1046.

766 **Lastovetsky OA, Gaspar ML, Mondo SJ, LaButti KM, Sandor L, Grigoriev IV,**
767 **Henry SA, Pawlowska TE. 2016.** Lipid metabolic changes in an early divergent
768 fungus govern the establishment of a mutualistic symbiosis with endobacteria.
769 *Proceedings of the National Academy of Sciences of the USA* **113**: 15102-15107.

770 **Leggett RM, Clavijo BJ, Clissold L, Clark MD, Caccamo M. 2014.** NextClip: an
771 analysis and read preparation tool for Nextera Long Mate Pair libraries.
772 *Bioinformatics* **30**: 566-568.

773 **Li H, Durbin R. 2009.** Fast and accurate short read alignment with Burrows-Wheeler
774 Transform. *Bioinformatics* **25**: 1754-1760.

775 **Li H, Handsaker B, Wysoker A, Fennell T, Ruan J, Homer N, Marth G, Abecasis**
776 **G, Durbin R, 1000 Genome Project Data Processing Subgroup. 2009.** The
777 Sequence alignment/map (SAM) format and SAMtools. *Bioinformatics* **25**: 2078-
778 2079.

779 **Lin K, Limpens E, Zhang Z, Ivanov S, Saunders DGO, Mu D, Pang E, Cao H, Cha**
780 **H, Lin T et al. 2014.** Single nucleus genome sequencing reveals high similarity
781 among nuclei of an endomycorrhizal fungus. *PLoS Genetics* **10**: e1004078.

782 **Lombard V, Golaconda Ramalu H, Drula E, Coutinho PM, Henrissat B. 2014.** The
783 carbohydrate-active enzymes database (CAZy) in 2013. *Nucleic Acid Research* **42**:
784 D490-D495.

785 **Luginbuehl LH, Oldroyd GED. 2017.** Understanding the arbuscule at the heart of
786 endomycorrhizal symbioses in plants. *Current Biology* **27**: R952-R963.

787 **Maeda T, Kobayashi Y, Kameoka H, Okuma N, Takeda N, Yamaguchi K, Bino T,**
788 **Shigenobu S, Kawaguchi M. 2018.** Evidence of non-tandemly repeated rDNAs and
789 their intragenomic heterogeneity in *Rhizophagus irregularis*. *Communications*
790 *Biology* **1**: 87.

791 **Maherali H, Klironomos JN. 2007.** Influence of phylogeny on fungal community
792 assembly and ecosystem functioning. *Science* **316** :1746-1748.

793 **Mathieu S, Cusant L, Roux C, Corradi N. 2018.** Arbuscular mycorrhizal fungi:
794 intraspecific diversity and pangenomes. *New Phytologist* **220**: 1129–1134.

795 **Martin FM, Uroz S, Barker DG. 2017.** Ancestral alliances: Plant mutualistic
796 symbioses with fungi and bacteria. *Science* **356**: eaad4501.

797 **Mittl PRE, Schneider-Brachert W. 2007.** Sell-like repeat proteins in signal
798 transduction. *Cellular Signalling* **19**: 20-31.

799 **Payen T, Murat C, Martin F. 2016.** Reconstructing the evolutionary history of gypsy
800 retrotransposons in the Périgord black truffle (*Tuber melanosporum* Vittad.).
801 *Mycorrhiza* **26**: 553–563.

802 **Pellegrin C, Morin E, Martin FM, Veneault-Fourrey C. 2015.** Comparative analysis
803 of secretomes from ectomycorrhizal fungi with an emphasis on small-secreted
804 proteins. *Frontiers in Microbiology* **6**: 1278.

805 **Price AL, Jones NC, Pevzner PA. 2005.** De novo identification of repeat families in
806 large genomes. *Bioinformatics* **21**: i351–i358.

807 **Redecker D, Schüssler A, Stockinger H, Stürmer SL, Morton JB, Walker C. 2013.**
808 An evidence-based consensus for the classification of arbuscular mycorrhizal fungi
809 (*Glomeromycota*). *Mycorrhiza* **23**: 515-531

810 **Riley R, Corradi N. 2013.** Searching for clues of sexual reproduction in the genomes
811 of arbuscular mycorrhizal fungi. *Fungal Ecology* **6**: 44-49.

812 **Ropars J, Toro KS, Noel J, Pelin A, Charron P, Farinelli L, Marton T, Krüger M,**
813 **Fuchs J, Brachmann A et al. 2016.** Evidence for the sexual origin of heterokaryosis
814 in arbuscular mycorrhizal fungi. *Nature Microbiology*. **1**: 16033.

815 **Salvioli A, Ghignone S, Novero M, Navazio L, Venice F, Bagnaresi P, Bonfante P.**
816 **2016.** Symbiosis with an endobacterium increases the fitness of a mycorrhizal
817 fungus, raising its bioenergetic potential. *ISME Journal* **10**: 130-44.

818 **Simão FA, Waterhouse RM, Ioannidis P, Kriventseva EV, Zdobnov EM. 2015.**
819 **BUSCO:** assessing genome assembly and annotation completeness with single copy
820 orthologs. *Bioinformatics* **31**: 3210–3212.

821 **Spanu PD. 2012.** The genomics of obligate (and nonobligate) biotrophs. *Annual Review*
822 *of Plant Pathology* **50**: 91-109.

823 **Spatafora JW, Chang Y, Benny GL, Lazarus K, Smith ME, Berbee ML, Bonito G,**
824 **Corradi N, Grigoriev I, Gryganskyi A et al. 2016.** A phylum-level phylogenetic
825 classification of zygomycete fungi based on genome-scale data. *Mycologia* **108**:
826 1028-1046.

827 **St-Arnaud M, Hamel C, Vimard B, Caron M, Fortin JA. 1996.** Enhanced hyphal
828 growth and spore production of the arbuscular mycorrhizal fungus *Glomus*
829 intraradices in an in vitro system in the absence of host roots. *Mycological Research*
830 **100**: 328–332.

831 **Stajich JE, Block D, Boulez K, Brenner SE, Chervitz SA, Dagdigian C, Fuellen G,**
832 **Gilbert JG, Korf I, Lapp H et al. 2002.** The Bioperl toolkit: Perl modules for the
833 life sciences. *Genome Research* **12**: 1611–1618.

834 **Stamatakis A. 2006.** RAxML-VI-HPC: maximum likelihood-based phylogenetic
835 analyses with thousands of taxa and mixed models. *Bioinformatics* **22**: 2688-2690.

836 **Strullu-Derrien C, Selosse MA, Kenrick P, Martin FM. 2018.** The origin and
837 evolution of mycorrhizal symbioses: from palaeomycology to phylogenomics. *New*
838 *Phytologist* **220**: 1012-1030.

839 **Sun X, Chen W, Ivanov S, MacLea, AM, Wight H, Ramaraj T, Mudge J, Harrison**
840 **MJ, Fei Z. 2018.** Genome and evolution of the arbuscular mycorrhizal fungus
841 *Diversispora epigaea* (*Glomus versiforme*) and its bacterial endosymbionts. *New*
842 *Phytologist*. doi: 10.1111/nph.15472.

843 **Tang N, San Clemente H, Roy S, Becard G, Zhao B, Roux C. 2016.** A survey of the
844 gene repertoire of *Gigaspora rosea* unravels conserved features among
845 glomeromycota for obligate biotrophy, *Frontiers in Microbiology* **7**: 233.

846 **Van der Heijden MGA, Martin FM, Selosse MA, Sanders IR. 2015.** Mycorrhizal
847 ecology and evolution: the past, the present, and the future. *New Phytologist* **205**:
848 1406–1423

849 **Tisserant E, Kohler A, Dozolme-Seddas P, Balestrini R, Benabdellah K, Colard A,**
850 **Croll D, Da Silva C, Gomez SK, Koul R et al. 2011.** The transcriptome of the
851 arbuscular mycorrhizal fungus *Glomus intraradices* (DAOM 197198) reveals
852 functional tradeoffs in an obligate symbiont. *New Phytologist* **193**: 755–769.

853 **Tisserant E, Malbreil M, Kuo A, Kohler A, Symeonidi A, Balestrini R, Charron P,**
854 **Duensing N, Frei dit Frey N, Gianinazzi-Pearson V et al. 2013.** Genome of an
855 arbuscular mycorrhizal fungus provides insight into the oldest plant symbiosis.
856 *Proceedings of the National Academy of Sciences of the USA* **110**: 20117-20122

857 **Uehling J, Gryganskyi A, Hameed K, Tschaplinski T, Misztal PK, Wu S, Desirò A,**
858 **Vande Pol N, Du Z, Zienkiewicz A, Zienkiewicz K et al. 2017.** Comparative
859 genomics of *Mortierella elongata* and its bacterial endosymbiont *Mycoavidus*
860 *cysteinexigens*. *Environmental Microbiology* **19**: 2964–2983.

861 **Voets L, de la Providencia IE, Declerck S. 2006.** Glomeraceae and Gigasporaceae
862 differ in their ability to form hyphal networks. *New Phytologist* **172**: 185-188.

863 **Wattam AR, Abraham D, Dalay O, Disz TL, Driscoll T, Gabbard JL, Gillespie JJ,**
864 **Gough R, Hix D, Kenyon R, Machi D et al. 2014.** PATRIC, the bacterial
865 bioinformatics database and analysis resource. *Nucleic Acids Research* **42**: D581-
866 D591.

867 **Wewer V, Brands M and Dörmann P. 2014.** Fatty acid synthesis and lipid metabolism
868 in the obligate biotrophic fungus *Rhizophagus irregularis* during mycorrhization of
869 *Lotus japonicus*. *Plant Journal* **79**: 398–412.

870 **Zeng T, Holmer R, Hontelez J, Te Lintel-Hekkert B, Marufu L, de Zeeuw T, Wu**
871 **F1, Schijlen E, Bisseling T, Limpens E. 2018.** Host- and stage-dependent
872 secretome of the arbuscular mycorrhizal fungus *Rhizophagus irregularis*. *Plant*
873 *Journal* **94**: 411–425.

The following Supporting Information is available for this article:

Supplementary Table S1 Summary statistics of predicted gene repertoires for Glomeromycotina, *Mortierella elongata*, and selected Mucoromycotina used in this study.

Supplementary Table S2 Number of fungal gene markers identified by BUSCO in the genome assemblies used in the present study.

Supplementary Table S3 Gene orthology for the the four sequenced Glomeromycotina and eight sequenced Mucoromycota species.

Supplementary Table S4 Summary statistics for predicted proteome, core and dispensable genes (core-disp) and species-specific genes (specs) of the eight Mucoromycota species.

Supplementary Table S5 Most abundant protein families in expansion in *Rhizophagus irregularis* compared to the other Glomeromycotina, selected Mucoromycotina and *Mortierella elongata*.

Supplementary Table S6 Most abundant protein families in expansion in *Rhizophagus cerebriforme* compared to the other Glomeromycotina, selected Mucoromycotina and *Mortierella elongata*.

Supplementary Table S7. Most abundant protein families in expansion in *Rhizophagus diaphanus* compared to the other Glomeromycotina, selected Mucoromycotina and *Mortierella elongata*.

Supplementary Table S8. Most abundant protein families in expansion in *Gigaspora rosea* compared to the other Glomeromycotina, selected Mucoromycotina and *Mortierella elongata*.

Supplementary Table S9. Distribution of genes coding for signaling/transduction pathways in Glomeromycotina species analyzed in this study.

Supplementary Table S10. List of orthologous genes showing evidence of rapid sequence evolution in the Glomeromycotina genomes.

Supplementary Table S11. Distribution of genes coding for secreted carbohydrate-active enzymes (CAZymes), total CAZymes and CAZymes acting on plant or fungal cell walls.

Supplementary Table S12. Presence of meiosis-specific gene orthologues in Glomeromycotina species with sequenced genomes and single nucleotide polymorphisms in Glomeromycotina.

Supplementary Table S13. Secretome, including secreted CAZymes, secreted lipases, secreted proteases and small secreted proteins (SSP) for all Mucoromycota species in this study.

Supplementary Table S14. Orthogroups of small secreted proteins without annotation (unknown proteins).

Supplementary Table S15. Presence and sequence similarity of upregulated genes from *R. irregularis* interacting with *Brachypodium distachyon* and of upregulated genes from *G. rosea* interacting with *Brachypodium distachyon* in genomes of sequenced Mucoromycota (linked to Fig. 5B).

Supplementary Table S16. Clusters of all Mucoromycota species genomes.

Supplementary Table S17. Pfam protein domains counts in genomes for all Mucoromycota species in this studies and five isolates of *R. irregularis* (linked to Fig.3A)

Supplementary Fig. S1 Macrosyteny between *Rhizophagus irregularis* and *R. diaphanus* scaffolds.

Supplementary Fig. S2 Expansion and contraction of gene families as identified by CAFÉ analysis in sequenced Glomeromycotina, *Mortierella elongata* and selected Mucoromycotina.

Supplementary Fig. S3 Sequence divergence of conserved orthogroups in sequenced Glomeromycotina in this study.

Supplementary Fig. S4 Presence and abundance of genes encoding secreted plant cell wall degrading enzymes in the genome of the eight Mucoromycota species.

Supplementary Fig S5 Distribution of allele frequency (as SNP) in the genome of *Rhizophagus irregularis*, *R. diaphanus*, *R. cerebriforme*, and *Gigaspora rosea*.

Supplementary Fig. S6 Schematic representation of the putative MAT-locus in Glomeromycotina.

Table 1 Summary statistics for genome assemblies of the sequenced Glomeromycotina and selected saprotrophic Mucoromycota used in this study.

Species	Assembly size (Mbp)	Contig no.	Contig N50 (no.)	Contig L50 (kbp)	Scaffolds	Scaffold N50	Scaffold L50 (kbp)	Scaffold (kbp) min - max		Total gap length (%)	Total repeat (%)	GC content (%)
<i>Gigaspora rosea</i>	597.95	28,997	3,991	37.7	7,526	734	232.08	0.92	1,204.75	7.92	63.44	28.81
<i>Mortierella elongata</i>	49.86	742	77	219.8	473	31	517.14	1.00	1,526.29	0.30	4.63	48.05
<i>Mucor circinelloides</i>	36.59	26	4	4318.34	26	4	4,318.34	2.29	6,050.25	0.00	20.38	42.17
<i>Phycomyces blakesleeanus</i>	53.94	350	41	370.4	80	11	1,515.58	2.96	4,452.46	1.06	9.74	35.78
<i>Rhizophagus cerebriforme</i>	136.89	14,636	1,679	18.5	2,592	266	147.87	0.90	709.02	17.60	24.77	26.55
<i>Rhizophagus diaphanus</i>	125.87	11,501	1,354	22.9	2,764	269	137.49	0.88	686.31	12.52	20.18	27.19
<i>Rhizophagus irregularis</i>	136.80	5,810	768	52.03	1,123	129	336.38	0.96	1,375.86	5.06	26.38	27.53
<i>Rhizopus microsporus</i>	25.97	823	111	69.4	131	8	1,118.34	1.02	2,782.17	2.41	4.68	37.48

Fig. 1 Distribution of transposable element (TE) families in genomes of sequenced Mucoromycota. (a) TE coverage (%) in genome assemblies. (b) Copy number per TE family.

Fig. 2 Organismal phylogeny of the eight Mucoromycota species, plus one representative of Basidiomycota (*Laccaria bicolor*), one representative of Ascomycota (*Tuber melanosporum*) and two basal fungi, *Conidiobolus coronatus* and *Rozella allomycis*. We identified 784 gene clusters with only one protein-coding gene per species by clustering protein sequences using FastOrtho (Wattam et al., 2013). Each cluster was then aligned with MAFFT (Katoh & Standley, 2002), and a maximum likelihood inference was performed with RAxML (PROTGAMMAWAG model) and 1000 bootstrap replicates (Stamatakis, 2014).

Fig. 3 Gene conservation and innovation in Glomeromycotina, Mortierellamycotina, Mucoromycotina species. (a) Organismal phylogeny. (b) Bar graphs represent sets of conserved proteins shared among species (dark blue), sets of duplicated conserved proteins shared among species (light blue), sets of dispensable proteins (purple), sets of duplicated dispensable proteins (light purple), species-specific (orange) and duplicated species-specific (light orange) proteins. Note that some of the species-specific genes found by comparing the eight Mucoromycota genomes have orthologues in other fungi (yellow). Protein ID and sequences for each FastOrtho orthogroups (i.e. gene families) are listed in Supporting Information Table S16.

Fig. 4 Functional diversity encoded by Mucoromycota genomes. (a) Presence and abundance of the different Pfam domain-containing proteins in the eight Mucoromycotina species (this study) and *Rhizophagus irregularis* isolates A1, A4, A5, B3 and C2 (Chen et al., 2018). The heat map depicts absolute Pfam domain counts in each of the sampled genomes, according to the color scale (only the top most frequent 100 domains are shown). The abundance values were then transformed into z-scores, which are measure of relative enrichment (red) and depletion (green); the hierarchical clustering was done with a Euclidian distance metric and average linkage clustering method. The data were visualized and clustered using MultiExperiment Viewer

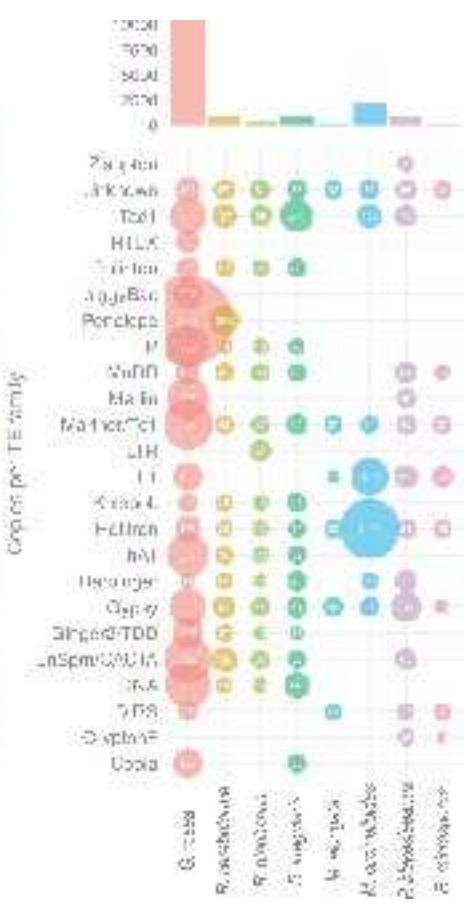
(<http://www.tm4.org/mev.html>). (b) Diversity of KEGG pathways in Mucoromycota genomes. Pearson correlation matrix was calculated based on profile of protein-coding genes assign to KEGG modules; to perform hierarchical clustering the correlation matrix is converted into a distance matrix. The hierarchical clustering was done with a Euclidian distance metric and complete linkage clustering method. Colors are coded from dark red representing high correlation to white representing lower correlation. Counts of selected Pfam-domain are listed in Supporting Information Table S17.

Fig. 5 Presence and abundance of genes encoding for secreted enzymes involved in the degradation of plant, fungal and bacterial cell wall polysaccharides in the eight Mucoromycota species. The bubble plot depicts absolute counts for genes encoding secreted CAZymes involved in the degradation of polysaccharides and lignin derivatives. The bar plots depicts the numbers and ratio of secreted and nonsecreted enzymes acting on plant (PCWDE) or microbial (MCWDE) polysaccharides (<http://www.cazy.org>). AA, auxiliary activities; CBM, carbohydrate-binding modules; CE, carbohydrate esterases; EXPN, distantly related to plant expansins; GH, glycoside hydrolases; PL, polysaccharide lyases.

Fig. 6 Presence and sequence similarity of symbiosis-upregulated genes from *Rhizophagus irregularis* (a) and *Gigaspora rosea* (b) interacting with *Brachypodium distachyon* in the genome of the eight Mucoromycota species. The heatmap depicts a double-hierarchical clustering of (a) 426 symbiosis-upregulated *R. irregularis* genes (rows, fold change ≥ 5 in symbiotic tissues compared to germinating hyphae from spores, false discovery rate-corrected $P \leq 0.05$; Supporting Information Table S15a) based on their percentage sequence identity, 0 to 100% (color scale at left) with their orthologues (if any) in selected taxa (columns). Right panel, functional categories (KOG) are given for each transcript cluster in percentage as bargrams and the number and percentage of genes in each cluster are shown. Data were visualized and clustered using R (package HeatPlus). The hierarchical clustering was done by using a Euclidian distance metric and Ward clustering method. The bottom heatmap (b) depicts a double-hierarchical clustering of 989 symbiosis-upregulated *G. rosea* genes (Table S15b) based on their percentage sequence identity with their orthologues (if any) in selected taxa.

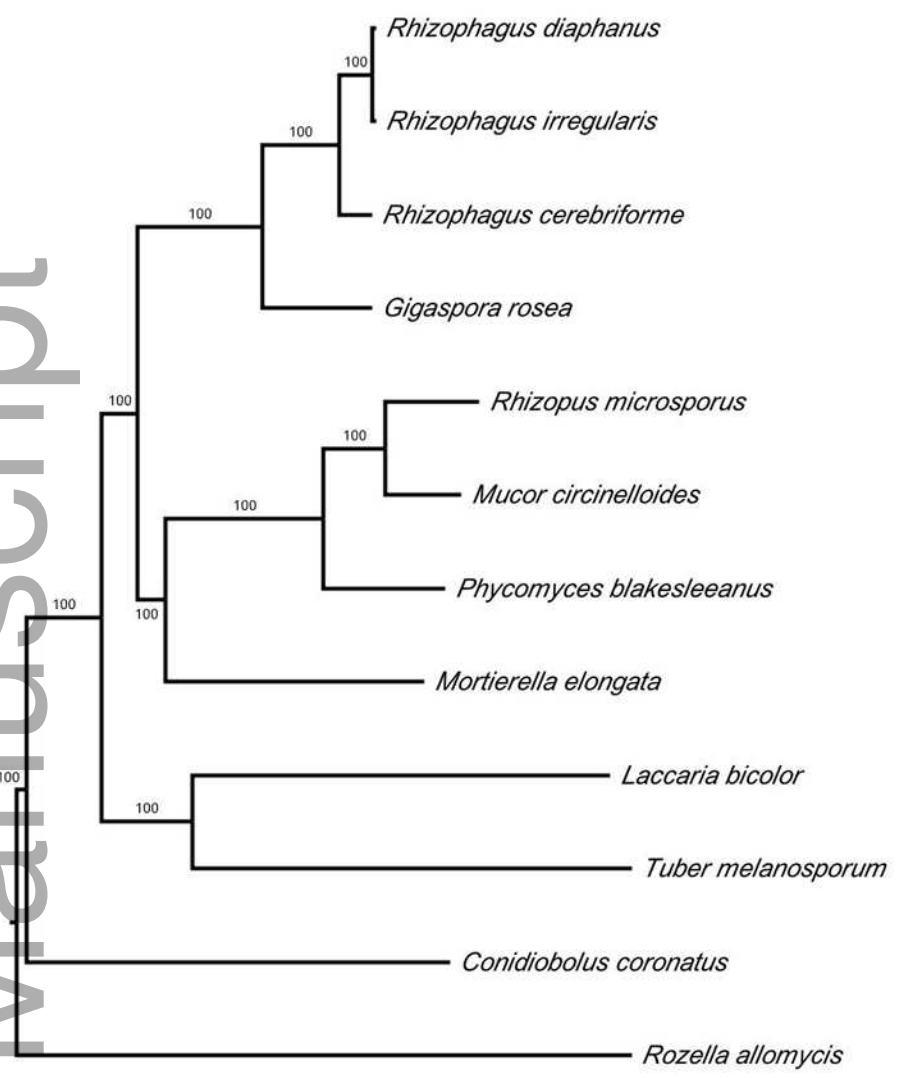
List of symbiosis-upregulated genes and their distribution by clusters is provided in Tables S15(a, b).

Author Manuscript



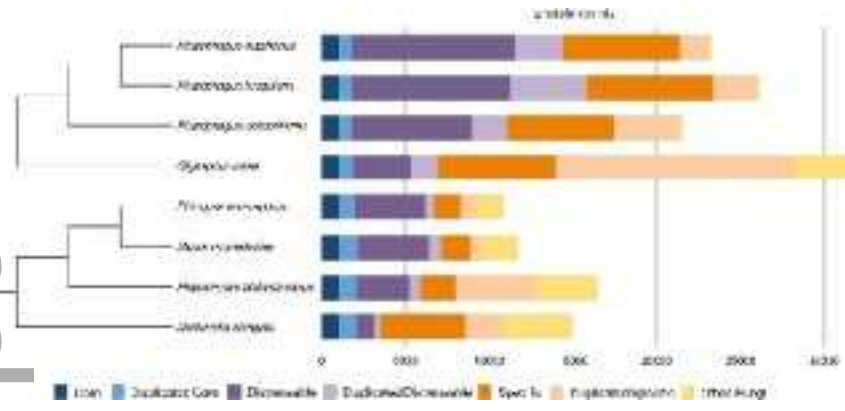
nph_15687_f1.tif

Author Manuscript

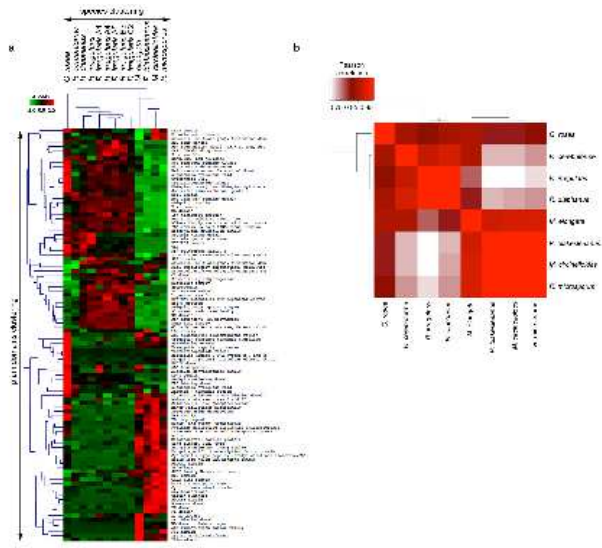


0.07

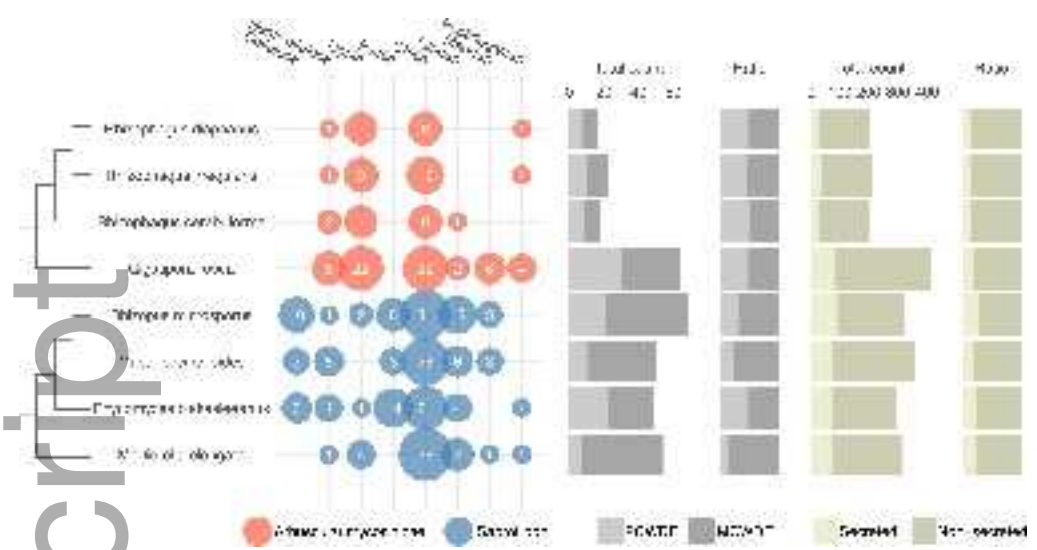
nph_15687_f2.tif



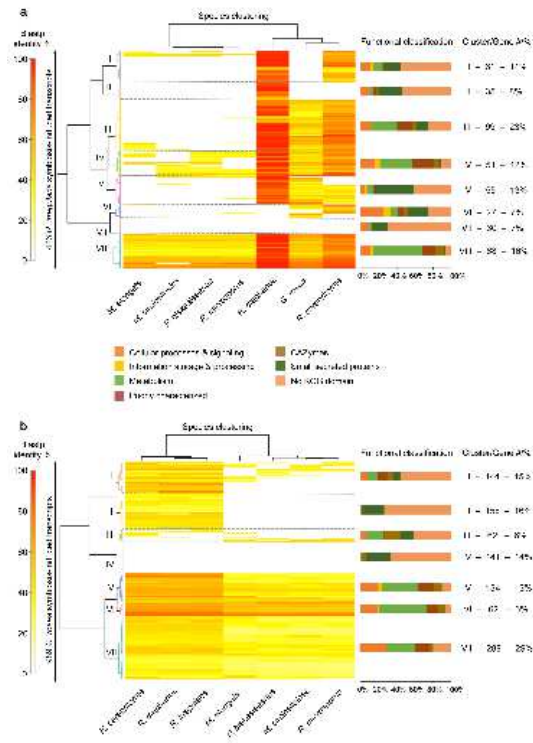
nph_15687_f3.tif



nph_15687_f4.tif



nph_15687_f5.tif



nph_15687_f6.tif